6th European Conference on Computational Mechanics (ECCM 6)
7th European Conference on Computational Fluid Dynamics (ECFD 7)
11 – 15 June 2018, Glasgow, UK

Electromechanical model of hiPSC-derived ventricular cardiomyocytes co-cultured with fibroblasts

A. Jung[1], **R. Frotscher**[1] **and M. Staat**[1]

[1] Aachen University of Applied Sciences, Campus Jülich
Institute of Bioengineering
Heinrich-Mußmann Str. 1, 52428 Jülich, Germany,
e.mail: {a.jung, frotscher, m.staat}@fh-aachen.de

Key Words: *Multi-scale model, FEM, Monodomain model, Electromechanical coupling, CellDrum*

Abstract. *The CellDrum provides an experimental setup to study the mechanical effects of fibroblasts co-cultured with hiPSC-derived ventricular cardiomyocytes. Multi-scale computational models based on the Finite Element Method are developed. Coupled electrical cardiomyocyte-fibroblast models (cell level) are embedded into reaction-diffusion equations (tissue level) which compute the propagation of the action potential in the cardiac tissue. Electromechanical coupling is realised by an excitation-contraction model (cell level) and the active stress arising during contraction is added to the passive stress in the force balance, which determines the tissue displacement (tissue level). Tissue parameters in the model can be identified experimentally to the specific sample.*

1 INTRODUCTION

Healthy cardiac tissue includes approximately 75% cardiomyocytes (CMs) by volume but CMs account for only 30-40% by cell number [1]. The majority of the other cells are the much smaller fibroblasts whose number even increases in aged tissue and in many forms of diseases [2].

Fibroblasts do not only contribute to the tissue structure but it has been shown in both experimental and computational studies that fibroblasts coupled to ventricular cardiomyocytes influence the electric conduction of cardiomyocytes, e.g. the action potential duration and the conduction velocity in tissue [2]-[10]. A computational study by Zhan *et al*. [9] suggests also consequences for the mechanical contraction of ventricular CMs. This is not surprising as the contraction is triggered by electrical activation via an intracellular calcium-dependent process called excitation-contraction coupling.

So far, experiments on the electrical effects of CM-fibroblast coupling have been performed with cardiac tissues obtained from various animal species [3][7][8]. Since the differentiation of human-induced pluripotent stem cells into CMs is a well-established methodology [11], the so-called human-induced pluripotent stem cell-derived cardiomyocytes (hiPSC-CMs) have become a promising alternative. They are harvested from somatic cells from mature donors, which increases their availability and ethical concerns become secondary for in-vitro testing [12]. On the plus side from a physiological point of view are e.g. a gene expression which is consistent with native human CMs [13], and the presence of the major ion current types seen

in native human CMs [14]. However, there exist also major structural, electrical, and mechanical differences to native human CMs [15]. These differences depend on the maturation state [16]-[21]. Maturation is promoted by time in culture [16], substrate stiffness [17], biochemical cues [18], external electrical stimulation [19], and an engineered longitudinally (anisotropic) alignment of the hiPSC-CM [20][21] while they are aligned randomly (isotropic). When drawing parallels to native human CMs in the interpretation of the experiments, all relevant differences need to be taken into account.

We use auto-contractile tissues of hiPSC-CMs on a highly flexible substrate to investigate the electrical and the mechanical effects of fibroblasts in cardiac tissue. In the tissue, nodal CMs assemble to a bundle and create an action potential which spreads over the tissue to trigger contraction of atrial and ventricular CMs. Multielectrode Array (MEA) technique is used to study the action potential and its propagation. Stiffness and contraction can be examined by the *CellDrum* device which was developed in our institute [22][23]. The *CellDrum* is a circular well ($d = 6.4$ mm) with a bottom formed by an ultra-thin ($t = 3 - 4$ µm) silicone membrane (substrate) on which the hiPSC-CM cell line is cultivated. HiPSC-CMs are aligned randomly in the tissue and mature by time in culture. The stiffness of the tissue construct (cardiac tissue and membrane) can be measured by inflation testing and the displacement and frequency of the contractions are recorded by a capacitive sensor.

Two co-cultured cell lines are used for the study: Cor.4VU® (Ncardia Germany, Cologne) containing 90% ventricular and 10% atrial and nodal hiPSC-CMs and Fibro.Cor.4U® (Ncardia Germany, Cologne). Fibroblasts Fibro.Cor.4U® are added with various relative cell amounts. In preliminary experiments [24], it was found that the tissue construct displacement was enhanced in the presence of fibroblasts with a relative cell content of up to 50%. This is in contradiction to the computational study of Zhan *et al*. [9] which suggested that the active stress of ventricular CMs (and thus their displacement) decreases when fibroblasts are added to the tissue.

Computational models can be used to interpret experimental data, provide mechanistic insights and translate experimental data to native human CMs. For these reasons, electromechanical multi-scale models of the *CellDrum* are developed. Frotscher et al. [25][26] published the first Finite Element Method (FEM) based models which were developed for a cell line with 5% nodal, 35% atrial, and 60% ventricular hiPSC-CMS (Cor.4U®, Ncardia Germany, Cologne) to study the effects of various cardiac drugs using the Hill equation [27][28]. Nodal, atrial, and ventricular cell models were implemented and the cells were considered to be homogeneosly distributed. Since electrical stimulation was driven by the nodal model in all points of the tissue construct, the propagation of the generated action potential at the tissue level was neglected.

Novel models consider only ventricular CMs because they make the largest part of the Cor.4VU® cell line. Electrical coupling of ventricular CMs and fibroblasts is taken into account and an external stimulation current is applied in the region of the nodal CM bundle to generate an action potential which then propagates through the tissue construct. As done already in previously published models [25][26], tissue related parameters can be adapted experimentally to the specific sample. Details of the novel computational models are given in this paper.

2 COMPUTATIONAL MODEL

2.1 Structure

The computational model of the *CellDrum* consists of two scales, the cellular and the tissue scale, and two physical phenomena, electricity and mechanics.

The cellular level consists of coupled electrical models of ventricular CMs and fibroblasts. They compute the membrane potential based on the ion currents across the membrane and the ventricular model additionally computes the membrane potential driven freely available calcium concentration inside the cell. The freely available calcium concentration is input for the mechanical (excitation-contraction) model which computes the active stress created by the ventricular CMs. Since nodal and atrial cells make only 10% of all cells in the investigated cell line, they are not considered in the electromechanical model. In consequence, pacemaker are missing and the ventricular cell model requires external stimulation.

The tissue construct is considered as one material which is, both electrically and mechanically, isotropic due to the random alignment of the hiPSC-CM on the silicone membrane. Electrical cell models are embedded in the reaction-diffusion type monodomain equation (monodomain model) which simulates the action potential propagation at the tissue level.
The active stress, which is computed by the cellular excitation-contraction model at each point of the tissue construct, is added to the passive stress in the force balance equation of the mechanical model (active stress model; [29]). This gives, for certain boundary conditions, the displacement of the beating tissue construct. The FEM is used to solve the models at the tissue level.

Tissue model parameter are adapted experimentally (conduction velocity measurements, inflation testing) to the specific sample and the validation of the *CellDrum* model is performed based on the central displacement of the tissue construct. An overview about the model and the workflow is displayed in **Fig. 1**.

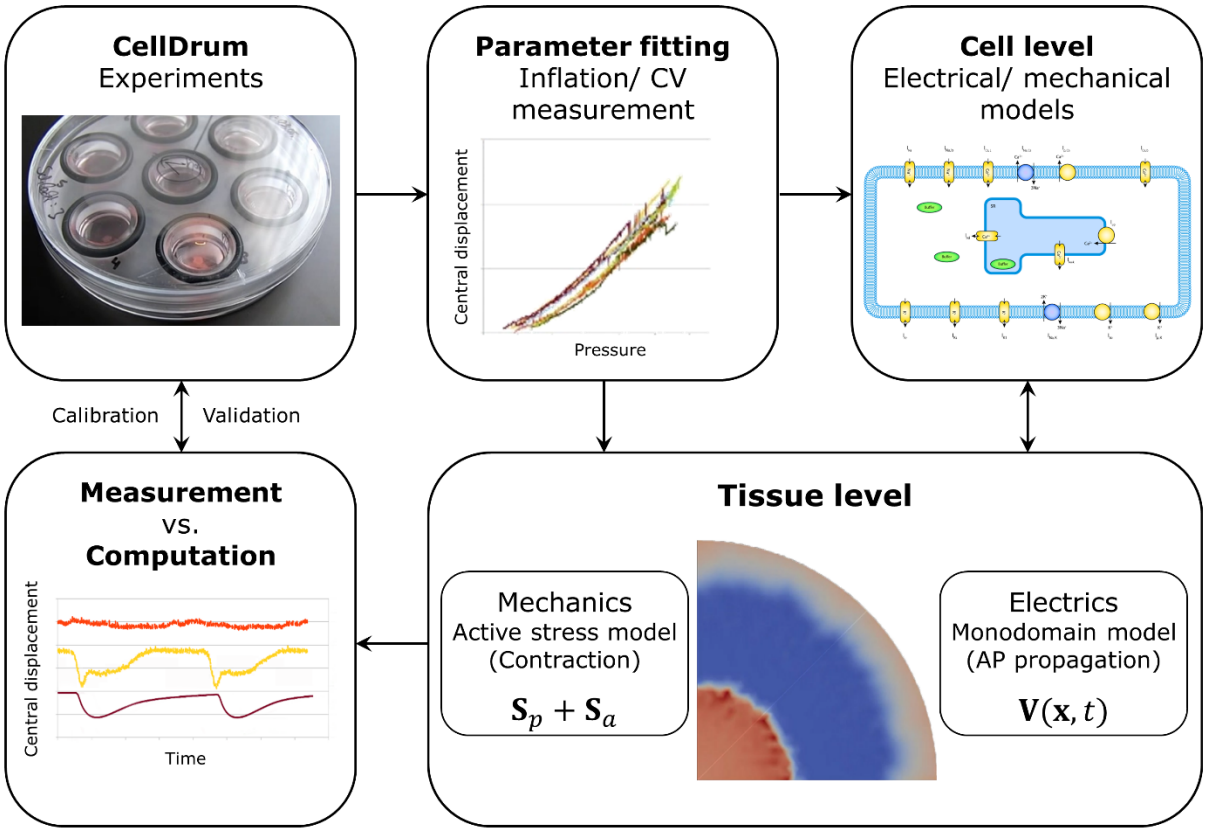

Fig. 1. Overview and workflow of the electromechanical *CellDrum* model.

2.2 Electrical model

Propagation of the action potential in cardiac tissue is described by the monodomain model [30]. The monodomain model is a simplified version of the bidomain model and is based on the assumption that the conductivity in the extracellular space is proportional to the intracellular conductivity. Potse *et al.* [31] compared both approaches and found the difference in conduction velocity to be negligibly small. The parabolic partial differential equation of the monodomain model reads

$$\frac{\partial V}{\partial t} = \nabla \cdot (\mathbf{D}\nabla \mathrm{V}) - I_{ion} \tag{1}$$

with the isotropic diffusion tensor

$$\mathbf{D} = D\mathbf{I} \tag{2}$$

and the no-flux (Neumann) condition at the boundaries of the tissue construct

$$\mathbf{n}(\mathbf{D}\nabla \mathrm{V}) = 0 \text{ on } \Gamma_N. \tag{3}$$

V denotes the membrane potential [mV], D is the diffusion coefficient [$\mathrm{mm^2ms^{-1}}$], $\mathbf{I}$ is the identity matrix, $\mathbf{n}$ is the outward normal, Γ is the boundary of the tissue construct, and I_{ion} is the total ion current density [$\mathrm{mA(mF)^{-1}}$] which is computed in the cell models. D is derived experimentally by linear conduction velocity measurements of the cell line using MEA. The initial value of the membrane potential $V(t_0)$ is in line with the ventricular cell model.

Couplings of ventricular cells and fibroblasts are assumed to be distributed homogeneously in the tissue.
Ventricular cell models used here, e.g. from ten Tusscher and Panfilov (native human CMs; [32]) or Paci *et al*. (hiPSC-CMs; [33]), are based on the Hodgkin-Huxley formulation [34]

$$\frac{\partial V}{\partial t} = -I_{ion}. \tag{4}$$

The total ion current density I_{ion} is the sum of the ion current densities I_i of all n channels across the membrane and the external stimulation current density I_{stim}

$$I_{ion} = I_{stim} - \sum_{i=1}^{n} I_i. \tag{5}$$

The stimulation current density is added in the elements belonging to the region of the nodal CM bundle.

Current densities of each ion channel i are a function of the maximum conductance G_i, a set of gate variables g_j, and the reversal potential E_i:

$$I_i = G_i \prod_{j=1}^{m} g_j (V - E_i). \tag{6}$$

The m gate variables of each ion channel control its opening and closure and α_j^+ and α_j^- are the respective opening and closure rates. They depend on a threshold value of the membrane potential:

$$\frac{\partial g_j}{\partial t} = \alpha_j^+(V)\left(1 - g_j\right) + \alpha_j^-(V) g_j. \tag{7}$$

The ordinary differential equations (ODEs) of the calcium, sodium, and potassium dynamics do not follow a general form in published ventricular CM models. Thus, for details, we refer to the original articles.

Fibroblasts are assumed to be homogenously distributed across the tissue, i.e. the same number of fibroblasts is coupled to each ventricular CM. Fibroblasts are resistively coupled to the ventricular CM by assigning an intercellular conductance G_{gap}. According to the fibroblast model of MacCannel *et al.* [4], the membrane potential of the fibroblast is given by

$$\frac{\partial V_f}{\partial t} = -I_f - \frac{G_{gap}(V_f - V_v)}{c_f}, \tag{8}$$

where f and v in the index denotes fibroblast and ventricular CM, respectively, and the membrane capacitance is denoted with c. A positive $I_{gap} = G_{gap}(V_f - V_v)$ indicates that current is flowing from the fibroblast into the CM.
The membrane potential of the ventricular CM is given similarly by

$$\frac{\partial V_v}{\partial t} = -I_v - \frac{n[G_{gap}(V_v - V_f)]}{c_v}. \tag{9}$$

The total number n of fibroblasts coupled to one ventricular CM is chosen with respect to the relative fibroblast cell content in the tissue. Corresponding to a homogenous distribution of fibroblasts, a relative fibroblast cell content of 25% for instance corresponds to $n = 0.3333$ $\left(\frac{25\%}{100\%} \cdot \frac{100\%}{100\% - 25\%}\right)$.
Four ion channels contribute to the total ion current density I_v in the fibroblasts. Thus, it is named an "active fibroblast model" whereas the "passive fibroblast model" consists of a membrane capacitance and ohmic resistance connected in parallel [4].

The tissue model is solved with the FEM and a fine mesh consisting of ten-node quadratic tetrahedral elements. The mesh remains unaltered during the simulation, i.e. deformations of the tissue construct due to the contraction of the ventricular CM are not considered in the electrical problem. Their effect on the conduction velocity was proven to be negligible small and substantial time savings could be achieved. Convergence of the conduction velocity was used as criterion to find the optimum element size in a sensitivity study.

The cell models are solved once in each element. The Rush-Larsen scheme [35] was used to solve the gating variable-ODEs of the ventricular cell model whereas the accuracy of the simple forward Euler method was proved to be sufficient for the other ODEs. The time step to solve the coupled electrical model was chosen to be $\Delta t = 0.1$ ms based on a sensitivity analysis with both conduction velocity and APD90 (90% of the action potential length) as criterions. To guarante convergence to steady state for a given contraction frequency, we paced the coupled cell model at the experimentally determined frequency for 50 beats and used the resulting values as initial conditions at t_0.

2.3 Mechanical model

The hyperelastic tissue construct is a solid body which, at time t_0, is in the reference configuration $\kappa_0(\mathcal{B})$ and has material points $\mathbf{X} \in \kappa_0(\mathcal{B})$. At t it is in the current configuration $\kappa_t(\mathcal{B})$ and the material points $\mathbf{x} \in \kappa_t(\mathcal{B})$ are mapped through the motion $\boldsymbol{\chi}(\mathbf{X}, t): \kappa_0(\mathcal{B}) \rightarrow \kappa_t(\mathcal{B})$ such that $\mathbf{x} = \chi_t(\mathbf{X}, t)$. The deformation gradient is defined to be

$$\mathbf{F} = \nabla_X \chi_t(\mathbf{X}, t) \tag{10}$$

and maps the unit tangents of the reference configuration onto those in the current configuration. The incompressible behaviour of the tissue construct is modeled by a multiplicative decomposition of the deformation gradient [36]

$$\mathbf{F} = \mathbf{F}_{vol}\bar{\mathbf{F}} \tag{11}$$

into the volume-changing (volumetric) part

$$\mathbf{F}_{vol} = J^{1/3}\mathbf{I} \tag{12}$$

and the volume-preserving (isochoric) part

$$\bar{\mathbf{F}} = J^{-1/3}\mathbf{F}, \tag{13}$$

where the volume ratio $J = \bar{\mathbf{F}} = 1$ is satisfied. The modified right Cauchy-Green tensor is

$$\bar{\mathbf{C}} = \bar{\mathbf{F}}^{\mathrm{T}}\bar{\mathbf{F}}. \tag{14}$$

Voigt´s isostrain condition is applied to guarantee equal kinematics for both the tissue and the membrane.

The force balance is given as

$$\nabla_X \cdot [\mathbf{F}\mathbf{S}(\bar{\mathbf{C}}, \mathbf{X})] + \mathbf{b}(\mathbf{X}) = 0, \tag{15}$$

where $\mathbf{S}$ is the second Piola-Kirchhoff stress tensor and $\mathbf{b}$ are the body forces per unit volume in the reference configuration.

On the boundary $\Gamma = \Gamma_D \cup \Gamma_N$, in the reference configuration of the tissue construct essential (Dirichlet) boundary conditions and natural (Neumann) boundary conditions are imposed:

$$\mathbf{U}(\mathbf{X}) = \bar{\mathbf{U}}(\mathbf{X}) \text{ on } \Gamma_D, \tag{16}$$

with a prescribed displacement $\bar{\mathbf{U}}(\mathbf{X})$, and

$$\mathbf{FS}(\mathbf{U},\mathbf{X})\mathbf{N}(\mathbf{X}) = \mathbf{T}(\mathbf{X}) \text{ on } \Gamma_N. \tag{17}$$

with the normal vector $\mathbf{N}$ and the prescribed surface traction $\mathbf{T}$. Dirichlet displacement boundary conditions are defined by the fixation of the membrane in the *CellDrum* and symmetry conditions are applied in order to compute the model only for one quarter of the circular tissue construct. The weight of the nutrient fluid given to the tissue defines the Neumann force boundary conditions.

The total stress $\mathbf{S}$ in the tissue construct is additively decomposed according to the active stress model:

$$\mathbf{S}(t) = \mathbf{S}_p + \mathbf{S}_a(t), \tag{18}$$

where $\mathbf{S}_p$ is the passive stress and $\mathbf{S}_a$ is the active stress. The passive stress of the isotropic tissue construct is written as

$$\mathbf{S}_p = 2\frac{\partial\psi(\mathbf{C})}{\partial\mathbf{C}} - p\mathbf{C}^{-1}, \tag{19}$$

with the neo-Hookean strain energy function

$$\psi = C_{10}(I_1 - 3), \tag{20}$$

where $I_1 = \mathrm{tr}\,\mathbf{C}$. The material parameter C_{10} is derived experimentally by inflation experiments.
The active stress of the ventricular CMs is assumed to act equally in all directions and is therefore written as

$$\mathbf{S}_a(t) = S_a(t)\mathbf{C}^{-1}, \tag{21}$$

where S_a is a time depending scalar value of the active stress computed by the cellular excitation-contraction model.

Excitation-contraction models used here, e.g. Land *et al*. (native human ventricular CMs, [37]), are based on ODEs of the form

$$\frac{\partial\boldsymbol{\zeta}}{\partial t} = f\left(\boldsymbol{\zeta}, Ca^{2+}, \lambda, \dot{\lambda}\right) = f\left(\boldsymbol{\zeta}, Ca^{2+}, \mathbf{C}, \dot{\mathbf{C}}\right), \tag{22}$$

$$S_a = f\left(\boldsymbol{\zeta}, \lambda, \dot{\lambda}\right) = f\left(\boldsymbol{\zeta}, \mathbf{C}, \dot{\mathbf{C}}\right), \tag{23}$$

where the states $\boldsymbol{\zeta}$ of the ventricular CM during active stress generation depend on the freely available calcium concentration Ca^{2+}, which is computed by the electrical ventricular cell model, the stretch λ of the ventricular CM and the stretch rate $\dot{\lambda}$ during contraction. We set stretch to a constant value of 1 and the stretch rate to zero. For details, we refer to the original articles. So far, there has no excitation-contraction model on hiPSC-CMs been published.

The tissue level is solved with the FEM and a mesh consisting of seven-node quadratic triangular shell elements. Compared to the element size of the electrical mesh, the element size of the mechanical mesh is much coarser. The central tissue construct displacement was chosen as criterion for the sensitivity analysis regarding the element size. The excitation-contraction model is solved together with the coupled electrical cell model, i.e. the scalar value of the active stress is computed in the elements of the electrical mesh. The classical 4th

order Runge-Kutta method is used to solve the ODEs and projection is applied to transfer the active stress value from the electrical to the mechanical mesh.

The time step to solve the mechanical tissue model was chosen to be $\Delta t = 1$ ms based on a sensitivity analysis with the time course of the central displacement as criterion, i.e. the mechanical tissue model is solved at every 10^{th} step of the electrical model.

Preliminary results of a similar model which contains the electrical ventricular cell model from ten Tusscher and Panfilov [32] and the excitation-contraction model from Niederer, Hunter and Smith [38] are published in Jung *et al*. [39].

3 LIMITATIONS

The computational model of the *CellDrum* has certain limitations which arise mainly from simplifications of the electromechanical modelling of the tissue construct, the cell models, and the modelling of the electromechanical interaction.

The tissue construct is electrically and mechanically considered as one material. This allows an easy sample specific tailoring of the strain energy function by inflation tests. However, this approach implies that the coupled electromechanical problem is solved also in the area of the silicon membrane which results in enhanced displacement. This inaccuracy decreases with increasing ratio between tissue thickness and membrane thickness.

The tissue construct is viscoelastic in reality. Cansiz *et al*. [40] has recently integrated a viscoelastic material model in a previously published electromechanically coupled computer model [41]. Viscoelasticity is however not included in the *CellDrum* model.

The electrical and mechanical tissue models can be adapted to the given sample in the experiments. This is however not yet possible for the cell models. A promising approach to tailor electrical models using the patch-clamp and optimal mapping techniques has recently been introduced by Lei *et al*. [42].

Since there is a lack of fibroblast and excitation-contraction models for hiPSC-CMS, a fibroblast model based on rat ventricular and native human atrial CMs [4] and a excitation-contraction model based on native human ventricular cells [37] were implemented.

Electromechanical interaction in CMs is not limited to the excitation-contraction coupling altough this is assumed in almost all computational models including ours. Excitation-contraction coupling describes the pathway from a given action potential to mechanical contraction and associated deformation. The opposite pathway does also exist, termed mechano-electric coupling: mechanical deformation can alter e.g. calcium dynamics, membrane potential, and conduction velocity. Comprehensive reviews including experimental and computational approaches to investigate mechano-electric coupling have been published by Kohl *et al*. [44] and Quinn and Kohl [45]. A detailed computational study has been published by Kuijpers *et al*. [46]. Membrane potential changes due to mechanical deformation have also been found in fibroblasts [7].

Furthermore, mechanical deformations can directly influence force production, termed

mechano-mechanical feedback [37][45][46]. This coupling is integrated in some excitation-contraction models including the chosen model developed by Land *et al*. [37]. However, we set the deformation in the *CellDrum* model to a constant value as the actual deformation computed by the mechanical tissue model is not transferred to the electrical model. Future work will evaluate the effects of a more detailed modelling of electromechanical interaction.

REFERENCES

[1] H.W. Vliegen, A. van der Laarse, C.J. Cornelisse and F. Eulderink, Myocardial changes in pressure overload-induced left ventricular hypertrophy. A study on tissue composition, polyploidization and multinucleation. *Eur. Heart J*., Vol. **12**, pp. 488-494, 2005.

[2] T. Kawara, R. Derksen, J.R. de Groot, et al., Acitvation delay after premature stimulation in chronically diseased human myocardium relates to the architecture of interstitial fibrosis. *Circulation*, Vol. **104**, pp. 3069-75, 2001.

[3] P. Camelliti, T.K. Borg, P. Kohl, Structural and functional characterization of cardiac fibroblasts. *Cardiovasc. Res*. Vol. **65**, pp. 40-51, 2005.

[4] K.A. MacCannell, H. Bazzazi, L. Chilton, Y., et al., A mathematical model of electrotonic interactions between ventricular myocytes and fibroblasts. *Biophys. J*., Vol. **92**, pp. 4121-4132, 2007.

[5] V. Jacquement, C.S. Henriquez, Modelling cardiac fibroblasts: interactions with myocytes and their impact on impulse propagation. *Europace*, Vol. **9**, vi29-37, 2007.

[6] A.R. Nayak, T.K. Shajahan, A.V. Panfilov, R. Pandit, Spiral-wave dynamics in a mathematical model of human ventricular tissue with myocytes and fibroblasts. *PLoS One*, Vol. **8**, e72950, 2013

[7] P. Kohl, P. Camelliti, F.L. Burton, G.L. Smith, Electrical coupling of fibroblasts and myocytes: relevance for cardiac propagation. *J. Electrocardiol*., Vol. **38**, pp. 45-50, 2005.

[8] P. Kohl, R.G. Gourdie, Fibroblast-myocyte eletrotonic coupling: does it occur in native cardiac-tissue. *J. Mol*. *Cell Cardiol*., Vol. **70**, pp. 37-46, 2014.

[9] H.Q. Zhan, L. Xia, G.F. Shou, et al., Fibroblast proliferation alters cardiac excitation conduction and contraction: a computational study. *J. Zhejing. Univ-Sci. B*., Vol. **15**, pp. 225-242, 2014.

[10] S. Sridhar, N. Vandersickel, A.V. Panvilov, Effect of myocyte-fibroblast coupling on the onset of pathological dynamics in a model of ventricular tissue. *Sci. Rep.*, Vol. **7**, 40985, 2017.

[11] X. Lian, J. Zhang, S. M. Azarin, K. Zhu, et al., Directed cardiomyocyte differentiation from human pluripotent stem cells by modulating wnt/β-catenin signaling under fully defined conditions. *Nat. Protoc.*, Vol. **8**, pp. 162-175, 2013.

[12] Y.L. Zheng, Some ethical concerns about human induced pluripotent stem cells. *Sci Eng Ethics*. Vol. **22**, pp. 1277-1284, 2016.

[13] S.J. Kattman, A.D. Witty, M. Gagliardi, et al., Stage-specific optimization of activin/nodal and bmp signaling promotes cardiac differentiation of mouse and human pluripotent stem cell lines. *Cell Stem Cell*, Vol. **8**, pp. 228-240, 2011.

[14] J. Ma, L. Guo, S.J. Fiene, et al., High purity human-induced pluripotent stem cell-derived cardiomyocytes: electrophysiological properties of action potentials and ionic currents. *Am. J. Physiol. Heart Circ. Physiol.*, Vol. **301**, H2006-H2017.

[15] C. Denning, V. Borgdorff, J. Crutchley, et al., Cardiomyocytes from human pluripotent stem cells: from laboratory curiosity to industrial biomedical platform. *Biochim. Biophys. Acta*, **1863**, pp. 1728-1748, 2016.

[16] M.L. McCain, A. Agarwal, H.W Nesmith, et al., Micromolded gelatin hydrogels for

extended culture of engineered cardiac tissues, *Biomaterials*, Vol. **35**, pp. 5462-5471, 2014.

[17] M.L. McCain, H. Yuan, F.S. Pasqualini, et al., Matrix elasticity regulates the optimal cardiac myocyte shape for contractility, *Am. J. Physiol. Heart Circ. Physiol*., Vol. **306**, H1525-39, 2014.

[18] X. Yang, L. Pabon, C.E. Murray, Engineering adolescence: maturation of human pluripotent stem cell-derived cardiomyocytes, *Cir. Res.*, Vol. **114**, pp. 511-523, 2014.

[19] G. Eng, B.W. Lee, L. Protas, et al., Autonomous beating rate adaption in human stem cell-derived cardiomyocytes, *Nat. Commun*., Vol. **7**, 10312, 2016.

[20] A.W. Feinberg, P.W. Alford, H. Jin, et al., Controlling the contractile strength of engineered cardiac muscle by hierachal tissue architecture, *Biomaterials*, Vol. **33**, pp. 5732-5741, 2012.

[21] S.P. Sheehy, A. Grosberg, P. Qin, et al., Toward improved myocardial maturity in an organ-on-chip platform with immature cardiac myocytes, *Exp. Biol. Med*., Vol. **242**, pp. 1643-1656, 2017.

[22] P. Linder, J. Trzewik, M. Rüffer, et al., Contractile tension and beating rates of self-exciting monolayers and 3D-tissue constructs of neonatal rat cardiomyocytes, *Med. Biol. Eng. Comput.*, Vol. **48**, pp. 59-65.

[23] M. Goßmann, R. Frotscher, P. Linder, et al., Mechano-pharmacological characterization of cardiomyocyte derived from human induced pluripotent stem cells. *Cell Physiol. Biochem*., Vol. **38**, pp. 1182-1192, 2016.

[24] A. Jung, R. Frotscher, M. Staat, Experimental and computational investigation of the electromechanical interaction between fibroblasts and hiPSC cardiomyocytes, Abstract Book, XXVI ISB Congress, Brisbane, Australia, p. 433, 2017.

[25] R. Frotscher, J.P. Koch, M. Staat, Computational investigation of drug action on human-induced stem cell-derived cardiomyocytes. *J. Biomech. Eng.*, Vol. **137**, 071002-7, 2015

[26] R. Frotscher, D. Muanghong, G. Dursun, et al., Sample-specific adaption of an improved elecro-mechanical model of in vitro cardiac tissue, *J. Biomech*., Vol. **49**, pp. 2428-2435, 2016.

[27] A.V. Hill, The possible effects of the aggregation of the molecules of haemoglobin on its dissociation curves, *J. Physiol*., Vol. **40**, pp. 4-7, 1910.

[28] J.N. Weiss, The Hill equation revisited: uses and misuses, *FASEB J*., Vol. **11**, pp. 835-841, 1997.

[29] D. Ambrosi, S. Pezzuto, Active stress vs. active strain in mechanobiology: constitutive issues, *J. Elast*., Vol. **107**, pp. 199-212, 2012.

[30] J.P. Keener, J. Sneysd, *Mathematical Physiology*. New York, Springer, 1998.

[31] M. Potse, B. Dubé, J. Richer, et al., A comparison of monodomain and bidomain reaction-diffusion models for action potential propagation in the human heart, *IEEE Trans. Biomed. Eng*., Vol. **53**, pp. 2425-2435, 2006

[32] K.H.W.J. ten Tusscher, A.V. Panfilov, Alternans and spiral breakup in a human ventricular tissue model, *Am. J. Physiol. Heart Circ. Physiol*., Vol. **291**, H1088-1100, 2006.

[33] M. Paci, J. Hyttinen, K. Aalto-Setälä, et al., Computational models of ventricular- and atrial-like human induced pluripotent stem cell derived cardiomyocytes. *Ann. Biomed. Eng.*, Vol. **41**, pp. 2334-2348, 2013.

[34] A.L. Hodgkin, A.F. Huxley, A quantitative description of membrane current and its application to conduction and excitation in nerve, *J. Physiol*., Vol. **117**, pp. 500-544, 1952.

[35] S. Rush, H. Larsen, A practical algorithm for solving dynamic membrane equations.

IEEE Trans. Biomed. Eng., Vol. **25**, pp. 389-392, 1978.
[36] P.J. Flory, Thermodynamic relations for highly elastic materials. *Trans. Faraday Soc.*, Vol. **57**, pp. 829-838, 1961.
[37] S. Land, S.J. Park-Holohan, N.P. Smith, et al., A model of cardiac contraction based on novel measurements of tension development in human cardiomyocytes. *J. Mol. Cell Cardiol*., Vol. **106**, pp. 68-83, 2017
[38] S.A. Niederer, P.J. Hunter, N.P. Smith, A quantitative analysis of cardiac myocyte relaxation: a simulation study. *Biophys J*., Vol. **90**, pp. 1697-1722, 2006.
[39] A. Jung, R. Frotscher, M. Goßmann, M. Staat, Modelling analysis of the effect of fibroblast on ventricular contraction. Abstract Book, VIII World Congress of Biomechanics, Dublin, Ireland, 2018.
[40] B. Cansiz, H. Dal, M. Kaliske, Fully coupled cardiac electromechanics with orthotropic viscoelastic effects. *Proc. IUTAM*, Vol. **12**, pp. 124-133, 2015.
[41] H. Dal, S. Göktepe, M. Kaliske, et al., A fully implicit finite element method for bidomain models of cardiac electromechanics. *Comp. Meth. Appl. Mech. Eng.*, Vol. **253**, pp. 323-336, 2013.
[42] C.L. Lei, K. Wang, M. Clerx, et al., Tailoring mathematical models to stem-cell derived cardiomyocyte lines can improve predictions of drug-induced changes to their electrophysiology. *Front. Physiol*., Vol. **8**, p. 986, 2017.
[43] P. Kohl, P. Hunter, D. Noble, Stretch-induced changes in heart rate and rhythm: clinical observations, experiments and mathematical models. *Prog. Biophys. Mol. Biol*., Vol. **71**, pp. 91-138, 1999.
[44] T.A. Quinn, P. Kohl, Rabbit models of cardiac mechano-electric and mechano-mechanical coupling. *Prog. Biophys. Mol. Biol*., Vol. **121**, pp. 110-122, 2016.
[45] N.H.L. Kuijpers, H.M.M ten Eikelder, P.H.M. Bovendeerd et al., Mechanoelectric feedback leads to conduction slowing and block in acutely dilated atria: a modeling study of cardiac electromechanics. *Am. J. Physiol. Heart Circ. Physiol*., Vol. **292**, H2832-H2853, 2007.